

Formation of nanoscale ferromagnetic MnAs crystallites in low-temperature grown GaAs

P. J. Wellmann,^{a)} J. M. Garcia, J.-L. Feng, and P. M. Petroff
Materials Department, University of California in Santa Barbara, Santa Barbara, California 93106

(Received 5 May 1997; accepted for publication 2 September 1997)

We report the formation of nanosize ferromagnetic MnAs crystallites imbedded in low-temperature grown GaAs using Mn⁺ ion implantation and subsequent annealing. The structural and magnetic properties of the crystallites have been characterized by transmission electron microscopy, electron beam induced x-ray fluorescence, and superconducting quantum interference device magnetometry. After an optimized thermal annealing at 750 °C, MnAs crystallites of 50 nm in size are formed. These nanomagnets show room temperature ferromagnetism. © 1997 American Institute of Physics. [S0003-6951(97)04343-X]

The formation of ferromagnetic nanosize particles (size ≈ 10–100 nm) imbedded in a semiconductor host^{1,2} and the growth of so called diluted magnetic semiconductor layers, such as MnAsGa on GaAs,^{3,4} are of particular interest due to their application in hybrid magnetic semiconductor devices. Typical device applications are magnetic field sensors, switches, and memories (see for example Refs. 5 and 6). The underlying physical effects relevant to the hybrid structures with nanosize magnets are the Hall effect, the anisotropic magnetoresistive (AMR), and the giant magnetoresistive (GMR) effects. Recently, Shi *et al.*¹ have shown the formation of MnGa ferromagnets imbedded in GaAs using Mn⁺ ion implantation and subsequent heat treatment. These particles exhibit room temperature ferromagnetism. De Boeck *et al.*² have reported the formation of MnAs crystallites in low-temperature (LT) GaAs introducing Mn during the molecular beam epitaxy MBE growth of the LT-GaAs layer. We have focused this study on the formation of MnAs crystallites in LT-GaAs using Mn⁺ ion implantation and subsequent annealing.

We have grown a 200- or 400-nm-thick LT-GaAs layer (substrate temperature 250 °C) on top of a 30 nm AlAs layer and a 500 nm GaAs buffer layer on a semi-insulating GaAs substrate. Mn⁺ ions have been implanted at an energy of $E = 180$ keV and a dose ranging from $1 \cdot 10^{14}$ to $1 \cdot 10^{16}$ cm⁻². TRIM computer simulations give rise to a Mn⁺ ion distribution within the 200 nm LT-GaAs layer. The calculated penetration depth R_p of the Mn⁺ ions is 110 nm, the distribution width ΔR_p is 50 nm. Rapid thermal annealing has been performed at 600–900 °C (5–180 s) under a forming gas atmosphere. The sample surface was covered with a 100 nm silicon nitride layer to prevent the evaporation of As during heat treatment. The structural properties have been investigated by transmission electron microscopy (TEM) and electron beam induced x-ray fluorescence (EDX). The magnetic properties have been characterized with a superconducting quantum interference device magnetometer (SQUID, $T = 1.7$ –400 K, $H = 0$ –±5 T). To reduce the diamagnetic background signal of the GaAs substrate, we have lifted off the LT-GaAs:Mn layer by selectively etching away the AlAs layer with hydrofluoric acid.⁷

Figure 1(a) shows the cross sectional TEM image of a sample annealed at 750 °C (5 s). The implanted Mn dose is $1 \cdot 10^{16}$ cm⁻². The bright stripe 200 nm below the surface marks the 30 nm AlAs which separates the 200 nm LT-

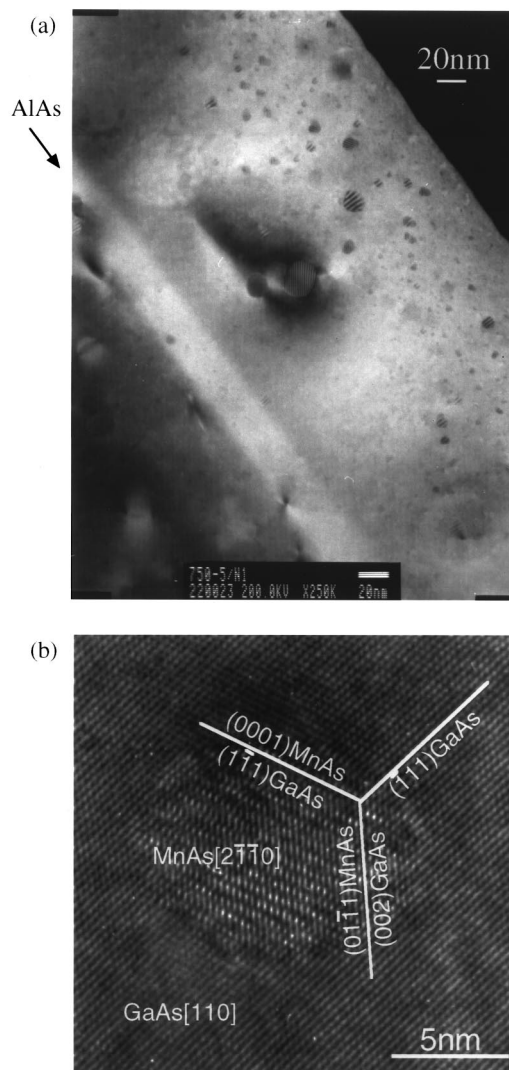


FIG. 1. (a) Cross sectional TEM image of LT-GaAs:Mn annealed at 750 °C (5 s) ($[\text{Mn}] = 1 \cdot 10^{16}$ cm⁻²). (b) High resolution TEM image of a single MnAs crystallite in LT-GaAs:Mn annealed at 750 °C (5 s) ($[\text{Mn}] = 1 \cdot 10^{16}$ cm⁻²).

^{a)}Electronic mail: wellmann@engineering.ucsb.edu

TABLE I. Atomic fraction of Ga, As, and Mn inside and outside a precipitate in LT-GaAs:Mn ($[Mn]=1 \cdot 10^{16} \text{ cm}^{-2}$) annealed at 750 °C (5 s).

	Ga [atom %]	As [atom %]	Mn [atom %]	Composition
LT-GaAs:Mn (outside precipitate)	52.6	46.7	0.7	GaAs
Precipitate	5.2	49.9	44.9	GaAs+MnAs
Precipitate B	25.7	46.3	27.9	GaAs+MnAs _{0.87} Ga _{0.13}

GaAs:Mn from the GaAs buffer layer. After annealing we find the formation of nanosize particles. The average particle volume corresponds to a particle size of 10 nm, the maximum size is up to 25 nm. Figure 1(b) shows a high resolution TEM image of such a precipitate. The annealing process is very efficient in recrystallizing the amorphized LT-GaAs. The surrounding of the precipitates show few interface dislocations. The diffraction pattern of these particles indicate an epitaxial relationship with the GaAs matrix [Fig. 1(b)]: $(0001)MnAs \parallel (1\bar{1}1)GaAs$ and $(01\bar{1}1)MnAs \parallel (002)GaAs$. Some smaller particles (size=2–5 nm) showed a different diffraction pattern; due to their small particle size it was not possible to estimate their epitaxial relationship with the GaAs matrix. However, larger MnAs crystallites (size>10 nm) tend to induce the formation of dislocations due to a slightly lattice mismatch between the precipitate and the GaAs matrix. Therefore the dislocation density remains in the order of 10^9 cm^{-2} after annealing. We have observed the formation of precipitates about 250 nm below the sample surface in the GaAs buffer layer. This layer has been grown at a substrate temperature of 600 °C and, unlike the LT-GaAs layer grown at 250 °C, contains no excess As. Therefore we exclude the presence of As precipitates in the GaAs buffer layer. We suggest an outdiffusion of Mn towards the GaAs substrate and the formation of Mn rich precipitates during the annealing process at 750 °C (5 s). No experimental data are available yet to support this hypothesis.

The chemical composition of the precipitates have been investigated by EDX measurements. We have used a small electron probe size (10 nm in diameter) to excite the x-ray fluorescence. Table I summarizes the results for the precipitate shown in Fig. 1(b). Taking into consideration the surrounding LT-GaAs matrix, we find that this precipitate exhibits Mn and As with a ratio of Mn:As=1:1, indicating that this particle is a MnAs crystallite. We also find that some precipitates contain a small amount of Ga (see precipitate B in Table I). Here the ratio of Mn:As is 1:0.6, indicating that precipitate B is a ferromagnetic phase of a $MnAs_nGa_m$ alloy. Another possibility, the presence of an antiferromagnetic Mn_2As phase, can be excluded from our magnetic measurements which show only ferromagnetic and superparamagnetic behavior.

We have carried out SQUID measurements of the magnetization $M(H)$ of LT-GaAs:Mn. Figure 2(a) shows the magnetization curves for various annealing conditions. The sample annealed at the lowest temperature (600 °C, 5 s) shows a small hysteresis loop. The magnetization does not saturate at high applied fields. This indicates that we have ferromagnetic particles in our LT-GaAs:Mn layer, but some particles may be too small in size (<1–2 nm) and give only

rise to a superparamagnetic background signal. As we increase the annealing temperature the hysteresis loop increases too and becomes maximum for annealing at 750 °C (5 s). Now the magnetization saturates at high applied magnetic fields ($H > 0.2 \text{ T}$) indicating that almost all Mn^{+} ions contribute to ferromagnetic crystallites. The Curie temperature T_c , which has been estimated from temperature dependent measurements of the remanence, is $T_c = 330 \pm 5 \text{ K}$. The value differs only slightly from bulk MnAs [$T_c(MnAs) = 318 \text{ K}$]. This confirms the result of the EDX measurement that the majority of the precipitates are MnAs crystallites.

As we increase the annealing temperature to 825 °C (5 s) and 900 °C (5 s) the saturation magnetization decreases [Fig. 2(a)]. One possible reason could be that a fraction of the Mn^{+} ions diffuse during the heat treatment out of the LT-

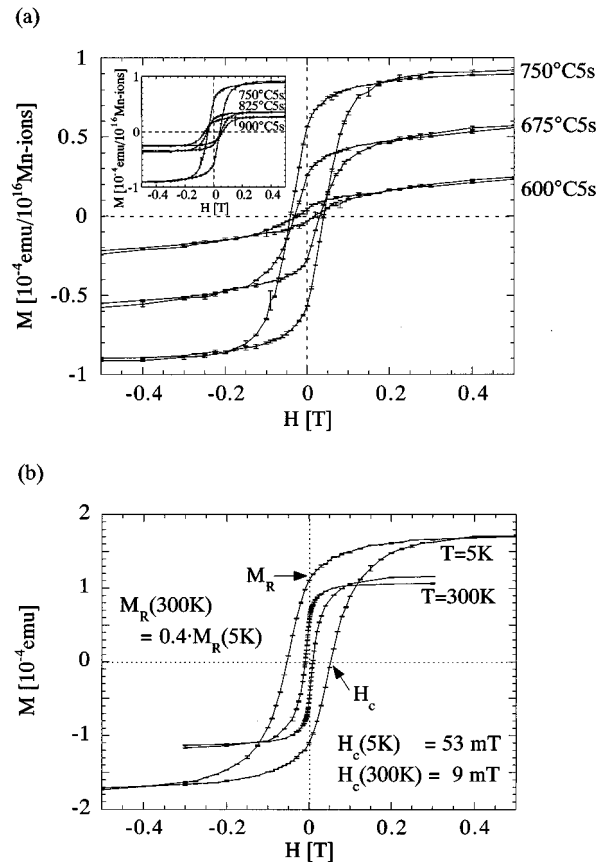


FIG. 2. (a) SQUID measurement at $T = 5 \text{ K}$ of the magnetization $M(H)$ of LT-GaAs:Mn ($[Mn]=1 \cdot 10^{16} \text{ cm}^{-2}$) for various annealing conditions ($T = 600\text{--}900 \text{ °C}$, 5 s). The magnetization $M(H)$ of each sample has been normalized to 10^{16} Mn ions. (b) SQUID measurement at 5 and 300 K of the magnetization $M(H)$ of LT-GaAs:Mn annealed at 750 °C (180 s) ($[Mn]=1 \cdot 10^{16} \text{ cm}^{-2}$).

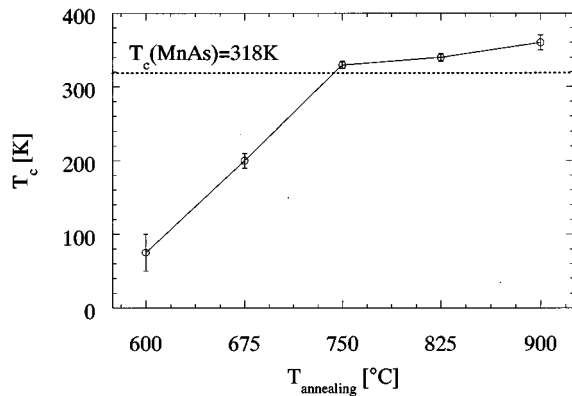


FIG. 3. Plot of the Curie temperature T_c of LT-GaAs:Mn ($[Mn]=1 \cdot 10^{16} \text{ cm}^{-2}$) vs the annealing temperature ($T=600\text{--}900 \text{ }^\circ\text{C}$, 5 s).

GaAs layer and into the GaAs buffer layer. We already mentioned the presence of some precipitates in the buffer layer when discussing the TEM image of the sample annealed at $750 \text{ }^\circ\text{C}$ (5 s) [Fig. 1(a)]. In addition we should point out that there is evidence for a change of the chemical composition of the crystallites at higher annealing temperatures which may cause a decrease of the saturation magnetization too.

In Fig. 3 we have plotted the evolution of the Curie temperature versus the annealing temperature. The Curie temperature increases rapidly from $T_c(600 \text{ }^\circ\text{C})=80 \text{ K}$ to $T_c(750 \text{ }^\circ\text{C})=330 \text{ K}$. We attribute this to the growth of the precipitates and to the formation of the MnAs phase. Starting at an annealing temperature of $750 \text{ }^\circ\text{C}$ the Curie temperature increases further, but now slowly from $T_c(750 \text{ }^\circ\text{C})=330 \text{ K}$ to $T_c(900 \text{ }^\circ\text{C})=360 \text{ K}$. This behavior is attributed to a change of the chemical composition of the precipitates. The EDX analysis already showed that the sample annealed at $750 \text{ }^\circ\text{C}$ contains some precipitates with a small amount of Ga (precipitate B in Table I). It is known from Shi *et al.*¹ that the Curie temperature of MnGa precipitates in GaAs [annealed at $920 \text{ }^\circ\text{C}$ (60 s)] have a value above 400 K. From this we conclude that in our experiment MnAs_nGa_m alloy precipitates may be formed at annealing temperatures higher than $750 \text{ }^\circ\text{C}$. The amount of Ga incorporated is supposed to increase with annealing temperature. The Curie temperatures of the MnAs_nGa_m particles are expected to be in between the values of MnAs ($T_c = 318 \text{ K}$) and MnGa ($T_c > 400 \text{ K}$).

For device applications of the MnAs nanosize ferromagnets imbedded in LT-GaAs, it is crucial to study the room temperature (RT) characteristics of the hysteresis loop.

Annealing at $750 \text{ }^\circ\text{C}$ for 5 s (without figure) yields a low room temperature coercivity [$H_c(5 \text{ K})=41 \text{ mT} \rightarrow H_c(300 \text{ K})=1 \text{ mT}$] and remanence [$M_R(300 \text{ K})=0.07 \cdot M_R(5 \text{ K})$]. By increasing the annealing time from 5 to 180 s we were able to increase the MnAs particle size from 10 to 50 nm and therefore enhance the coercivity and remanence. Figure 2(b) shows the magnetization curves of a sample annealed at $750 \text{ }^\circ\text{C}$ for 180 s. An increase of the room temperature coercivity by a factor of 9 is observed [$H_c(5 \text{ s})=1 \text{ mT} \rightarrow H_c(180 \text{ s})=9 \text{ mT}$]. It is remarkable that the room temperature remanence M_R remains 40% of the low temperature value. The conductivity of the LT-GaAs:Mn layer annealed at $750 \text{ }^\circ\text{C}$ (180 s) is $110 \Omega^{-1} \text{ cm}^{-1}$. The reported values of the coercivity, remanence, and conductivity make the MnAs nanosize crystallites imbedded in LT-GaAs possible candidates for hybrid ferromagnetic semiconductor devices if the diffusion of Mn is adequately controlled or used.

In conclusion we have reported the formation of nanosize ferromagnetic MnAs crystallites in LT-GaAs using Mn^+ ion implantation and subsequent heat treatment. We have investigated the structural and the magnetic properties by TEM, EDX, and SQUID measurements. The best formation conditions of the MnAs crystallites in LT-GaAs:Mn are rapid thermal annealing at $750 \text{ }^\circ\text{C}$. The MnAs crystallites exhibit room temperature ferromagnetism. These nanomagnet characteristics could open the way to novel hybrid magnetic semiconductor structures.

We would like to thank D. D. Awschalom for fruitful discussions. This work has been supported by QUEST, an NSF Science and Technology center (Grant No. DMR91.20007). P.J.W. is a postdoctoral fellow of the Deutsche Forschungsgemeinschaft (DFG) J.M.G. is a postdoctoral fellow of the Spanish Ministry of Education and Science.

- ¹J. Shi, J. M. Kikkawa, R. Proksch, T. Schaeffer, D. D. Awschalom, G. Medeiros-Ribeiro, and P. M. Petroff, *Nature (London)* **377**, 707 (1995); J. Shi, J. M. Kikkawa, D. D. Awschalom, G. Medeiros-Ribeiro, P. M. Petroff, and K. Babcock, *J. Appl. Phys.* **79**, 5296 (1996).
- ²J. De Boeck, R. Osterholt, A. Van Esch, H. Bender, C. Bruynseraede, C. Van Hoof, and G. Borghs, *Appl. Phys. Lett.* **68**, 2744 (1996).
- ³H. Ohno, A. Shen, F. Matsakura, A. Oiwa, A. Endo, S. Katsumoto, and Y. Iye, *Appl. Phys. Lett.* **69**, 363 (1996).
- ⁴T. Hayashi, M. Tanaka, T. Nishinaga, and H. Shimada, *J. Appl. Phys.* **81**, 4865 (1997).
- ⁵J. De Boeck, T. Sands, J. P. Harbison, A. Scherer, H. Gilchrist, T. L. Cheeks, M. Tanaka, and V. G. Keramidas, *Electron. Lett.* **29**, 421 (1993).
- ⁶J. M. Daughton, *Thin Solid Films* **216**, 162 (1992).
- ⁷E. Yablonovitch, T. Gmitter, J. P. Harbison, and R. Bhat, *Appl. Phys. Lett.* **51**, 2222 (1987).